

# Investigation of the Impact of Different Materials on the Efficiency of Lead-free Perovskite Solar Cell

MOSTAFA SALAH<sup>1,\*</sup>, MENNA ELKOMY<sup>1</sup>, OMAR MOHAMED<sup>1</sup>, MOHAMED HAMOUDA<sup>2</sup>,  
MARINA SOBHY<sup>1</sup>, MOHAMED MOUSA<sup>1</sup>

<sup>1</sup>Electrical Engineering Department,  
Future University in Egypt,  
Cairo 11835,  
EGYPT

<sup>2</sup>Independent Electricity System Operator (IESO),  
Ontario M5H 1T1,  
CANADA

**Abstract:** - A solar cell is an electrical device that converts light energy into electrical energy via the photovoltaic effect. Sometimes called a photovoltaic cell or PV cell. In essence, a solar cell is a p-n junction diode. Solar cells are a type of photoelectric cell, which is characterized as an apparatus that changes its electrical properties in response to light, including resistance, voltage, and current. Organic-inorganic halide-based perovskite solar systems are getting closer to commercialization and have become more efficient. Because lead-based perovskite materials have toxicity issues, the scientific community has recently become interested in lead-free alternatives. A lead-free n-i-p based planar heterostructure perovskite solar cell made of intrinsic-CH<sub>3</sub>NH<sub>3</sub>SnI<sub>3</sub> methyl ammonium tin iodide (MASnI<sub>3</sub>) as an i- and p-layer Spiro-OMeTAD with SnO<sub>2</sub> for the n layer is optimized for device efficiency using SCAPS numerical simulation. The 3<sup>rd</sup> layer (electron layer) is modified with an efficiency of 2.03%, with another material SnO<sub>2</sub>, as the efficiency increased to 2.62%, V<sub>oc</sub> of 0.6428V, J<sub>sc</sub> = 6.44 mA/cm<sup>2</sup>, and FF of 63.40% are achieved. After that the cell layers of the cell are optimized to achieve the highest efficiency of 10.13%.

**Key-Words:** - ETM, Lead-free Perovskite solar cell, PSC, power conversion efficiency, PCE; optimization.

Received: May 16, 2024. Revised: November 19, 2024. Accepted: December 15, 2024. Published: February 19, 2025.

## 1 Introduction

One of the environmental problems resulting from energy scarcity is the search for more affordable, less polluting energy sources. Coal and oil are currently the most extensively used energy sources worldwide, yet. They are also the main contributors to hazardous effluent emissions and CO<sub>2</sub> depletion.

Due to these energy sources' limitations, people's focus has shifted to renewable energy sources, [1], [2], [3]. The need for clean energy is growing worldwide, but when source availability is considered, the sun will emerge as the most dependable alternative energy source because of its low maintenance requirements, zero emissions, and noise levels. Furthermore, to lower the high cost of power grid extension, it may be a good choice for distributed electrification. Of all the renewable energy sources, photovoltaic (PV) energy appears to be the most significant and a good option for reducing damaging environmental effects like carbon

dioxide emissions. Direct conversion of light into electricity is possible with PV cells. They are also regarded as an environmentally friendly option for producing electricity close to load centers. PV systems are currently essential for producing electricity, and their use is expanding quickly. Crystalline silicon, thin-film silicon, amorphous silicon, Cu (InGa)Se<sub>2</sub>, and cadmium are common types of solar cells. Telluride, dye-sensitized, organic, and multi-junction solar cells, [4], [5], [6].

Perovskite solar cells are a promising class of solar cells that have attracted a lot of interest in the past 10 years due to their numerous benefits, including low exciton binding energy, tunable bandgap, high absorption coefficient, strong bipolar charge mobility, long carrier diffusion length, and low trap state density. Based on lead (Pb) perovskites, PSCs' power conversion efficiency (PCE) has significantly increased, going from 3.8% to a newly certified value of 25.2%. These Pb-based high-efficiency PSCs (MAPbI<sub>3</sub>, FAPbI<sub>3</sub>,

$\text{Cs}_{0.05}\text{FA}_{0.85}\text{MA}_{0.10}\text{Pb}(\text{I}_{0.97}\text{Br}_{0.03})_3$  do, however, have some inevitable drawbacks, such as the fact that lead is hazardous to the environment and living things and is difficult for the body to expel, [7], [8], [9].

In this study, we reviewed the changes in the efficiency by changing the parameters of the materials with constant thickness and doping. With the highest efficiency material, we start to change in thickness and doping of material to see the changes happening in efficiency of each layer. The rest of this paper is organized as follows section 2 is all about methods and material used, section 3 shows our work and results taken. Finally, Section 4 is a conclusion about our work.

## 2 Methods and Materials

The University of Gent in Belgium's Department of Electronics and Information Systems (ELIS) created the one-dimensional solar cell simulation tool known as SCAPS (a Solar Cell Capacitance Simulator). Windows comes with a 1D solar cell modeling application called SCAPS.

It operates better than other solar device simulators and produces encouraging simulation results. The behavior of the suggested design was numerically simulated in this simulation investigation using SCAPS.

The program was based on the continuity equations for charge carriers (electrons and holes), Poisson's equation, which relates the total space charge density to the divergence of the electric field  $E$ , and the carrier transport equations, which relate the behavior of the carrier concentrations  $p$  and  $n$  and the electric field. These semiconductor equations are formulated as follows.  $N_D$  and  $N_A$  for the doping densities of donors and acceptors, respectively.  $G$  and  $R$  for generation and recombination rates.  $J_n$  and  $J_p$  for electron and hole current densities.  $\mu_n$  and  $\mu_p$  for the mobilities of electrons and holes.  $D_p$  and  $D_n$  for the corresponding diffusion coefficients.

$$J_n = q(n\mu_n E + D_n \nabla_n) \quad (1)$$

$$J_p = q(p\mu_p E + D_p \nabla_p) \quad (2)$$

$$\epsilon \nabla \cdot E = \rho \quad (3)$$

$$\rho = q(p - n + N_A^- + N_D^+) \quad (4)$$

By considering boundary conditions, SCAPS solves these equations in one dimension to determine the steady-state response. Using SCAPS, the following steps are used to evaluate a PV cell's performance. First, a validation procedure was run to match the experimental cell's results with the simulated ones, [10]. The structure of the lead-free

perovskite solar cell (LF-PSC) is illustrated in Figure 1(a). Fluorine-doped tin oxide (FTO) is utilized as a transparent conducting oxide (TCO). Nanoporous titanium dioxide ( $\text{TiO}_2$ ) is utilized as an electron transport material (ETM).  $\text{Cs}_2\text{SnI}_4\text{Br}_2$  is utilized as the absorber layer. Copper thiocyanate ( $\text{CuSCN}$ ) is utilized as hole transport material (HTM). The parameters of the utilized are listed in Table 1.

Next, the program was utilized to ascertain the PV cell's current voltage characteristics in the light illumination. Numerous metrics, including generation, recombination rates, energy band diagrams,  $J_{SC}$ , FF, PCE, and  $V_{OC}$  can be computed. These electrical measurements for AC and DC can be reproduced and generated under various temperatures and illumination levels, regardless of whether the cell is in the dark or the light.

SCAPS offers several benefits, including the capacity to simulate up to seven distinct films and the creation of multiple cells structures.

Secondly, different ETMs are utilized but with constant thickness and doping showing its parameters in Table 2. SCAPS is used to get the highest efficient material by drawing JV and the QE curves.  $\text{SnO}_2$ -based cell has the highest efficiency. Therefore, we started using this layer.

Table 1. The used materials parameters of the LF-PSC

	CuSCN	Perovskite	TiO <sub>2</sub>
<b>Thickness (nm)</b>	200	400	50
<b>E<sub>g</sub>(eV)</b>	2.1	1.4	3.20
<b>χ(eV)</b>	3.4	4.11	4.3
<b>ε<sub>r</sub></b>	3	9	10
<b>μ<sub>e</sub></b>	1	10	200
<b>μ<sub>h</sub></b>	10	10	50
<b>N<sub>c</sub>(cm<sup>-3</sup>)</b>	2.5E18	2.2E18	1E20
<b>N<sub>v</sub>(cm<sup>-3</sup>)</b>	1.8E19	1.9E19	1E20
<b>N<sub>a</sub>(cm<sup>-3</sup>)</b>	0	0	10 <sup>17</sup>
<b>N<sub>A</sub>(cm<sup>-3</sup>)</b>	1E16	1E14	0

Table 2. The used materials parameters of different ETMs

	SnO <sub>2</sub>	WS <sub>2</sub>	ZnO	IGZO	Zn <sub>0.85</sub> Mg <sub>0.15</sub> O	ZnO <sub>0.3</sub> S <sub>0.7</sub>
<b>E<sub>g</sub>(eV)</b>	3.5	1.8	3.3	3.05	3.55	3.07
<b>χ(eV)</b>	4	3.95	3.9	4.16	3.75	3.84
<b>ε<sub>r</sub></b>	9	13.6	9	10	9	9
<b>μ<sub>e</sub></b>	20	100	50	15	50	100
<b>μ<sub>h</sub></b>	10	100	5	0.1	20	25
<b>N<sub>c</sub>(cm<sup>-3</sup>)</b>	2.2E10 <sup>17</sup>	2.2E10 <sup>17</sup>	10 <sup>19</sup>	5E10 <sup>18</sup>	9E10 <sup>16</sup>	2.2E10 <sup>18</sup>
<b>N<sub>v</sub>(cm<sup>-3</sup>)</b>	2.2E10 <sup>16</sup>	2.2E10 <sup>16</sup>	10 <sup>19</sup>	5E10 <sup>18</sup>	9E10 <sup>17</sup>	1.8E10 <sup>18</sup>

After that, the cell is optimized to increase the cell's efficiency. Firstly, by changing the thickness, and the doping of the transport layers. Moreover, the work functions of the front and back contacts are investigated. After that, we worked on the absorber layer (perovskite) by changing the doping. Thickness, and defect density ( $N_t$ ).

### 3 Results and Discussion

#### 3.1 Initial Conditions

The lead-free perovskite solar cell gave out a PCE of 2.03% using default layers. The main layer that was focused on to improve this efficiency was the ETM layer.  $TiO_2$  was the initial material for the ETM layer where it gave an efficiency of 2.03%,  $V_{oc}$  0.57 Volt equals to,  $J_{sc}$  equals to 6.24  $mA/cm^2$ , and Fill factor equals to 57.53% as extracted from Figure 1(b).

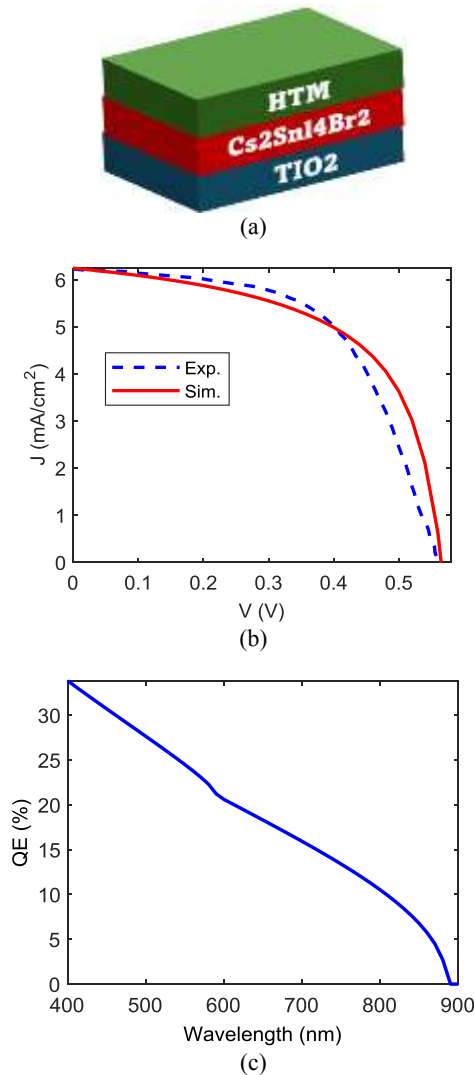


Fig. 1: (a) Structure of the calibrated LF-PSC, (b) JV curves of the simulated cell Vs the experimental cell, and (c) QE of the simulated cell

#### 3.2 Different ETMs

To improve the cell efficiency a modification was made by replacing the  $TiO_2$  with other materials having different parameters with the same thickness and doping level.

$Zn_{0.85}Mg_{0.15}O$  material gave out an efficiency of 2.33%,  $V_{oc}$  of 0.64 v,  $J_{sc}$  of 6.4  $mA/cm^2$ , and a FF of 56.69% as deduced from Figure 2.

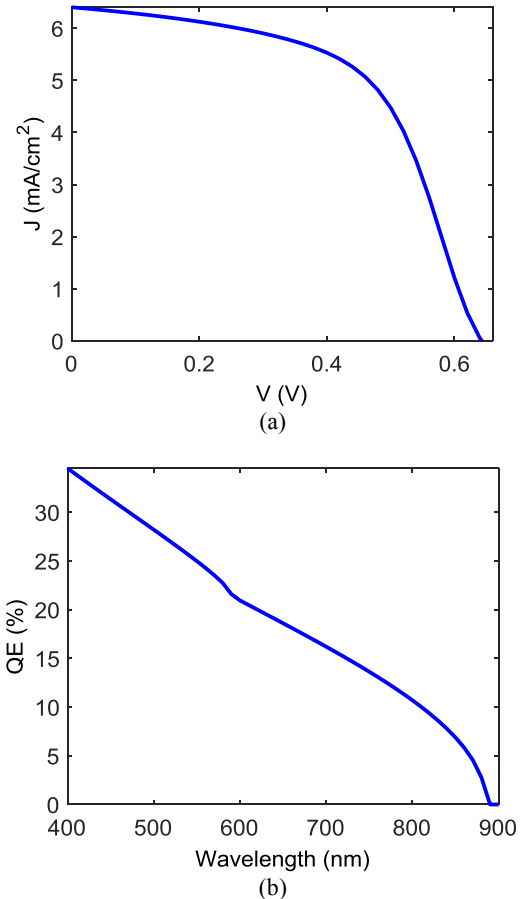
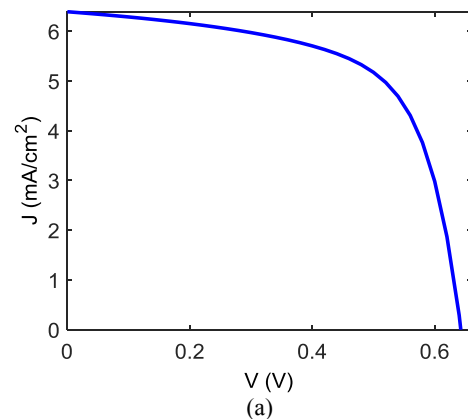


Fig. 2:  $Zn_{0.85}Mg_{0.15}O$ -based cell a)JV, and b) QE.

$ZnO_{0.3}S_{0.7}$  material gave out an efficiency of 2.59%,  $V_{oc}$  of 0.64 V,  $J_{sc}$  of 6.39  $mA/cm^2$  with FF of 63.01% as extracted from Figure 3.



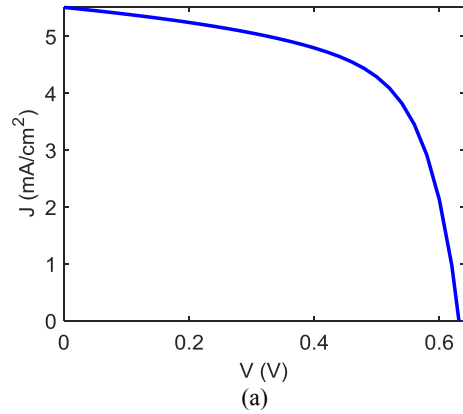
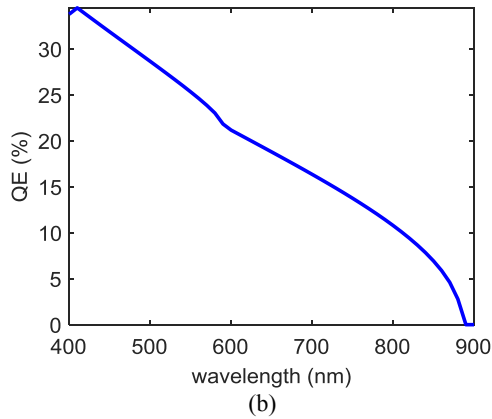


Fig. 3: ZnO<sub>0.3</sub>S<sub>0.7</sub>-based cell a) JV, and b) QE

Figure 4 shows using SnO<sub>2</sub> material with efficiency of 2.62%, V<sub>oc</sub> 0.64 v, J<sub>sc</sub> 6.44 mA/cm<sup>2</sup> with FF 63.4%.

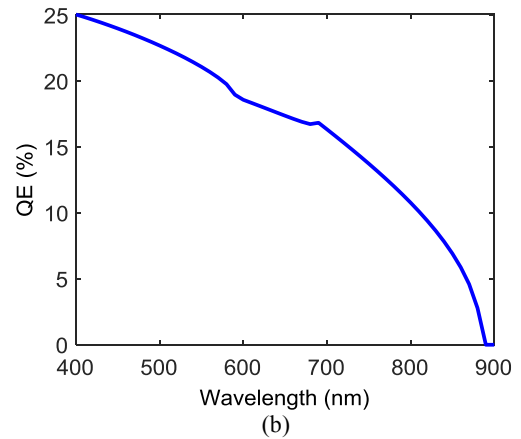
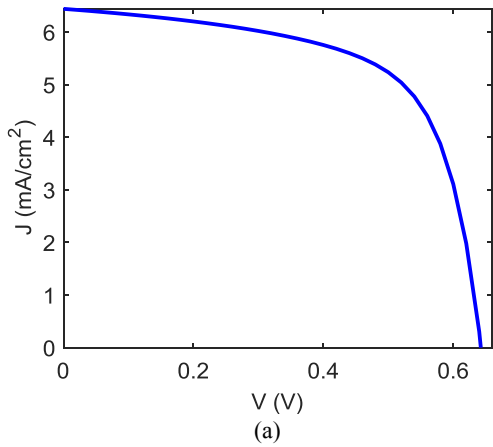


Fig. 5: WS<sub>2</sub>-based cell a) JV, and b) QE

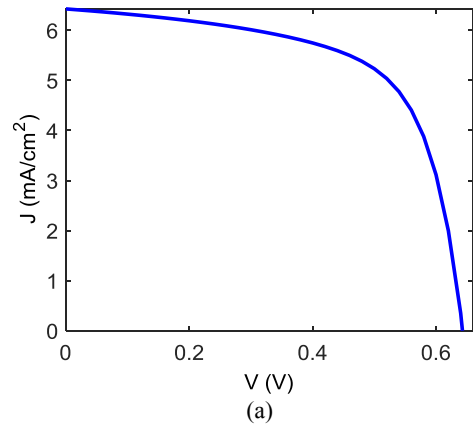
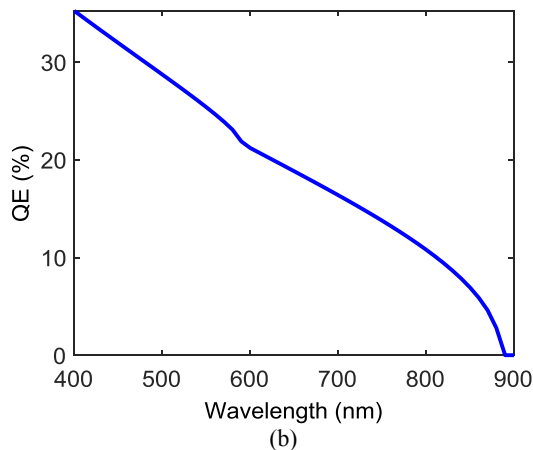


Fig. 4: SnO<sub>2</sub>-based cell a) JV, and b) QE

Using WS<sub>2</sub> material gives out an efficiency of 2.14%, V<sub>oc</sub> 0.63 V, J<sub>sc</sub> 5.51 mA/cm<sup>2</sup> and FF 61.56% as can be deduced from Figure 5.

Using ZnO material JV and QE curves are given in Figure 6 with efficiency of 2.62%, V<sub>oc</sub> of 0.64 V, J<sub>sc</sub> of 6.43 mA/cm<sup>2</sup> and FF 63.46%.

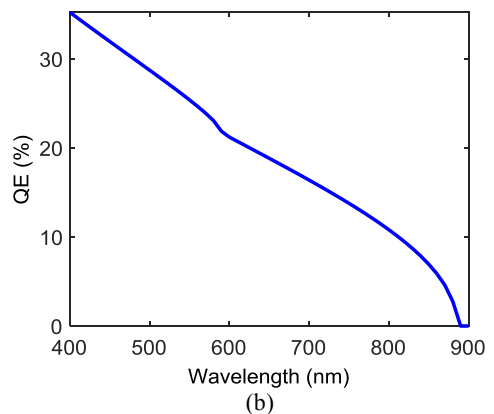


Fig. 6: ZnO-based cell a) JV, and b) QE

IGZO material gave out an efficiency of 2.44%,  $V_{oc}$  of 0.63 volt,  $J_{sc}$  of 6.34 mA/cm<sup>2</sup> and FF 61.21% as can be extracted from Figure 7.

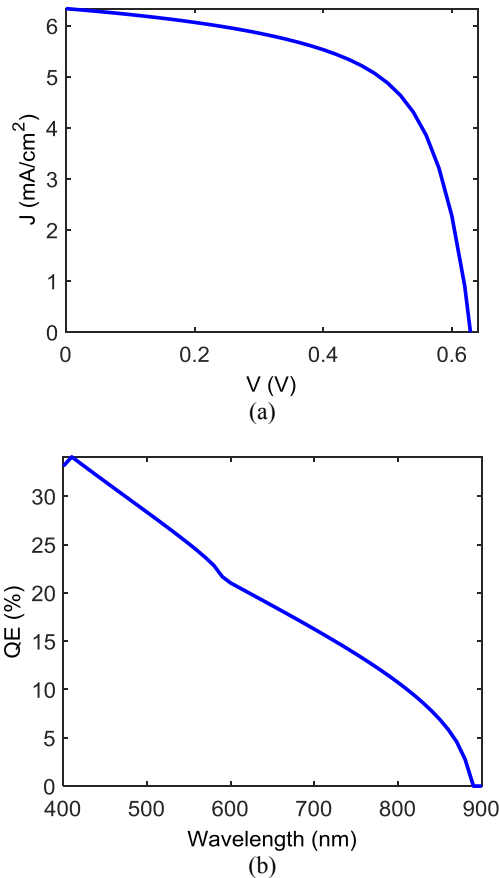


Fig. 7: IGZO-based cell a) JV, and b) QE

### 3.3 Cell Optimization

a) *The SnO<sub>2</sub> material Optimization:* The SnO<sub>2</sub> material was chosen as it had the highest efficiency which is equal to 2.62%. Then, that material had been modified to increase the cell's efficiency. First by changing the thickness then by changing the doping. Figure 8 and Figure 9 show the output factors that had been affected by thickness and doping, respectively. The highest efficiency was 2.65% at a SnO<sub>2</sub> thickness of 200 nm, and the highest efficiency was 2.75% at a doping concentration of  $1 \times 10^{18}$  cm<sup>-3</sup>.

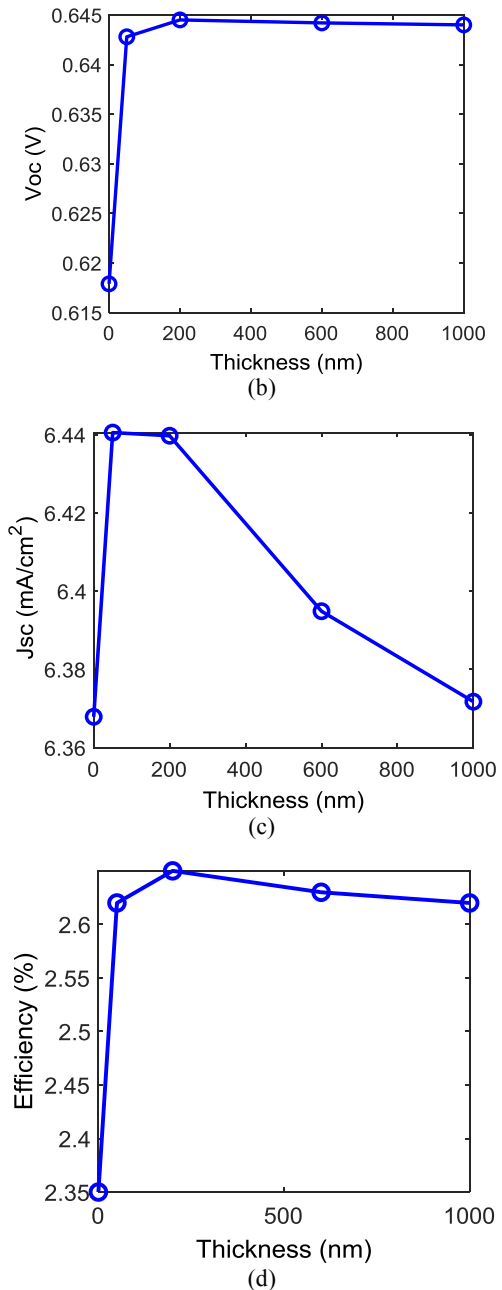
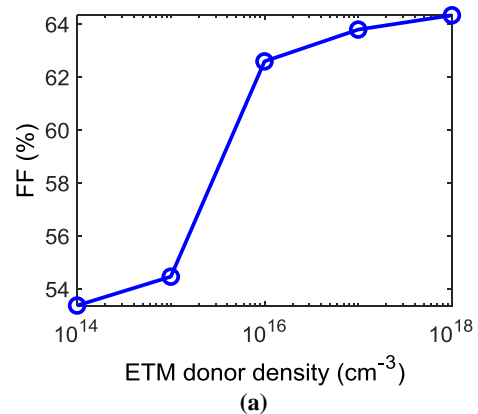
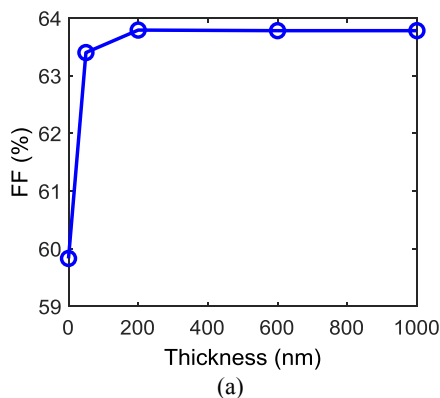


Fig. 8: SnO<sub>2</sub>-based cell performance parameters' variations with the ETM thickness (a) FF, (b)  $V_{oc}$ , (c)  $J_{sc}$ , and (d) efficiency



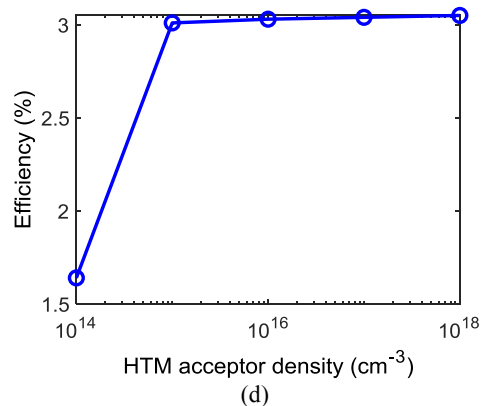
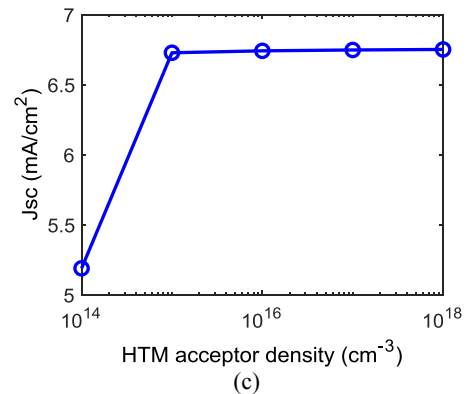
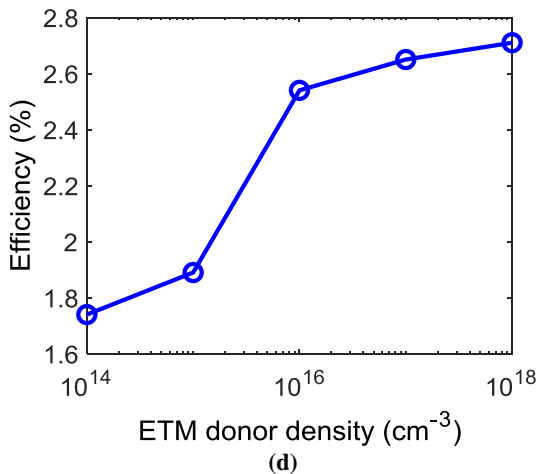
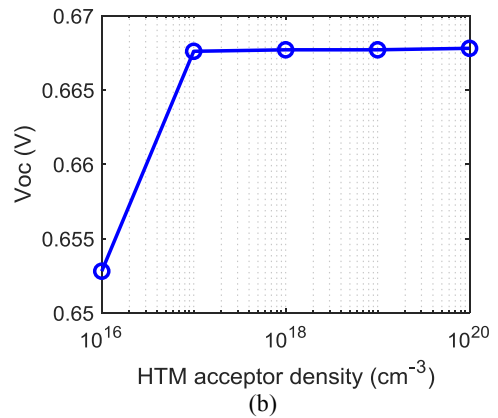
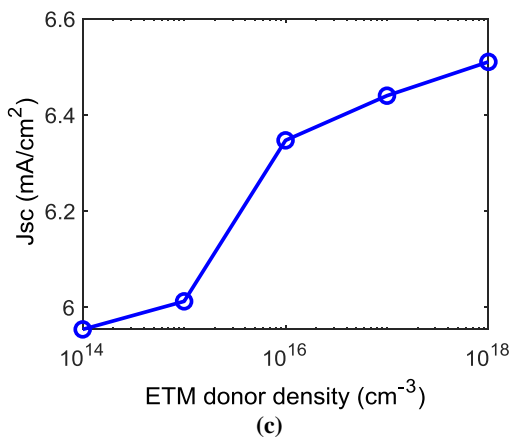
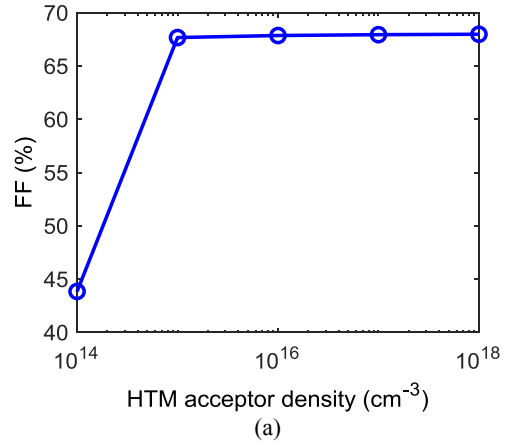
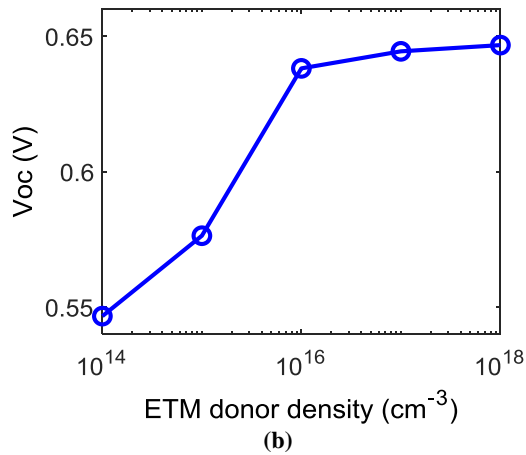
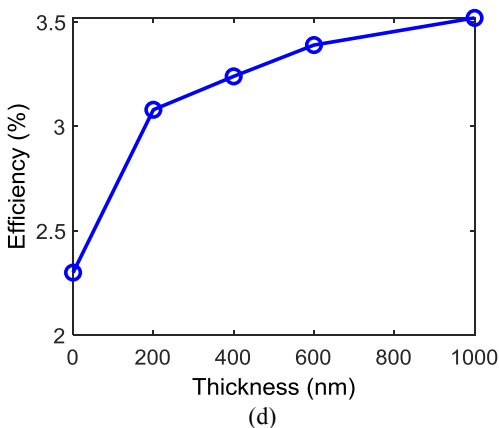
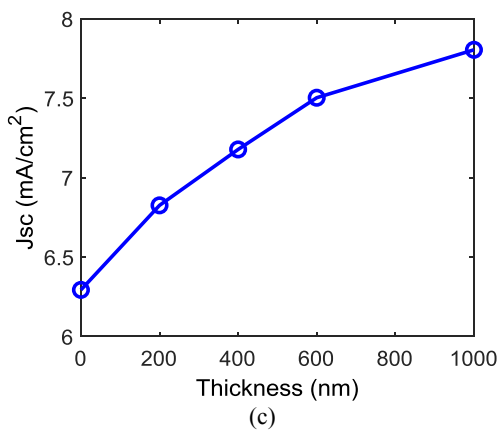
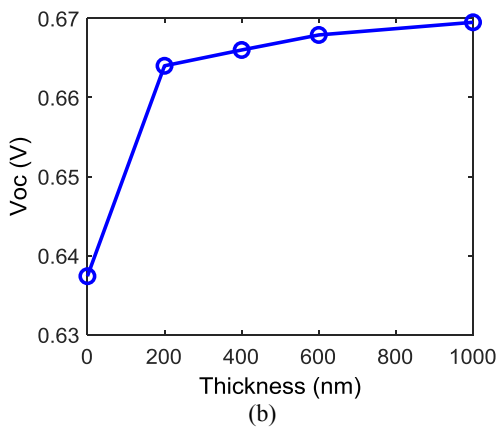
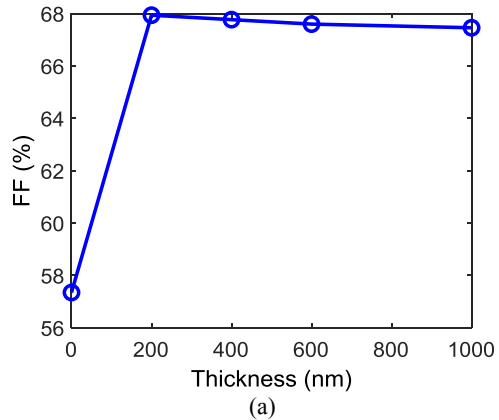


Fig. 9: SnO<sub>2</sub>-based cell performance parameters' variations with the ETM doping (a) FF, (b) Voc, (c) JSC, and (d) efficiency

*b) HTM Optimization:* In the second step, to increase the efficiency we worked on the HTM by changing the doping and the thickness as shown in Figure 10 and Figure 11, respectively. The highest efficiency was found at doping concentrations of 10<sup>18</sup> cm<sup>-3</sup> and 1000 nm.

Fig. 10: SnO<sub>2</sub>-based cell performance parameters' variations with the HTM doping (a) FF, (b) Voc, (c) Jsc, and (d) efficiency



*c) Back Contact and Front Contact Optimization:* Figure 12 and Figure 13 show how the performance parameters are affected by the work function of the back and front contacts, respectively. The Highest efficiency was 3.15% at a back contact work function of 5.75 eV and the highest efficiency was 7.23% at a front contact work function of 3.5 eV.

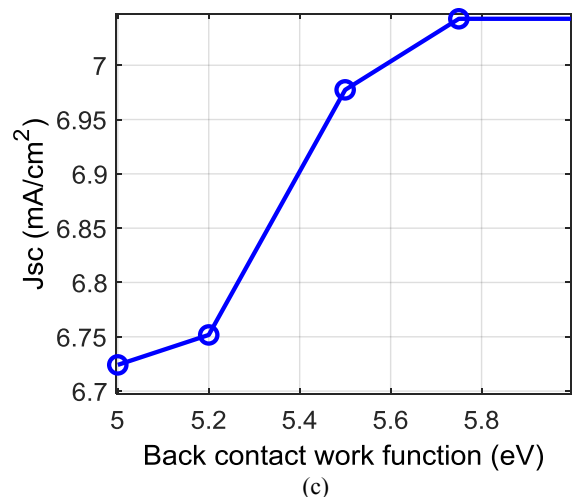
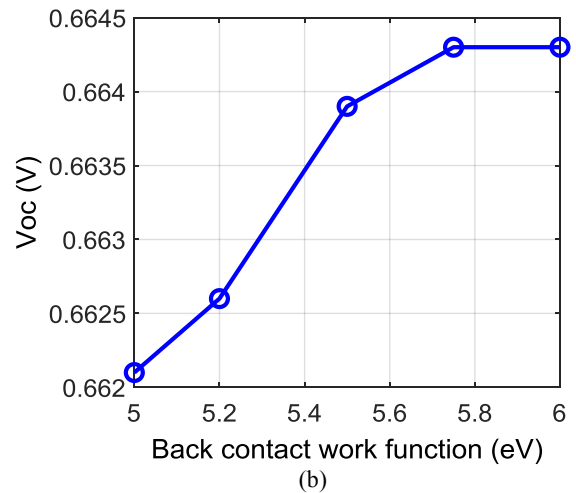
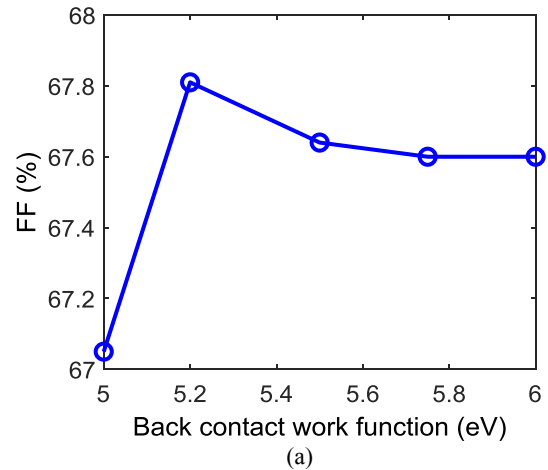


Fig. 11: SnO<sub>2</sub>-based cell performance parameters' variations with the HTM thickness (a) FF, (b) Voc, (c) JSC, and (d) efficiency

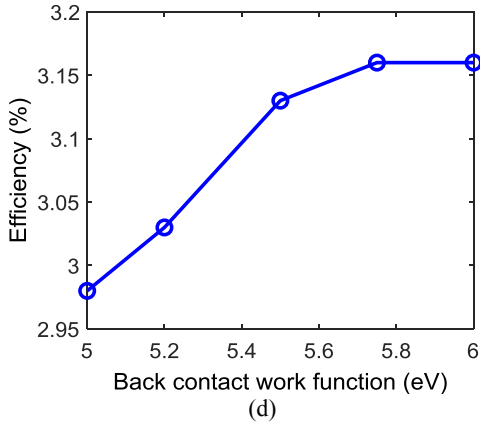


Fig. 12: SnO<sub>2</sub>-based cell performance parameters' variations with the back contact work function thickness (a) FF, (b) V<sub>oc</sub>, (c) J<sub>sc</sub>, and (d) efficiency

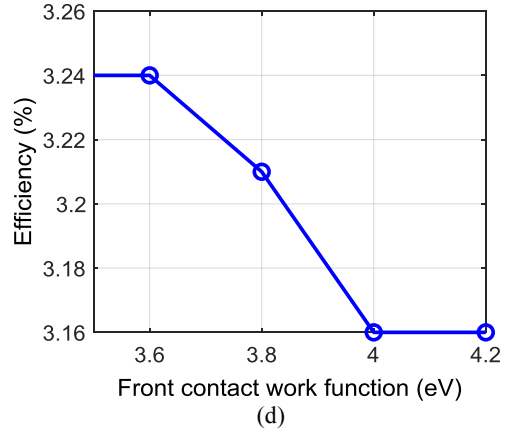
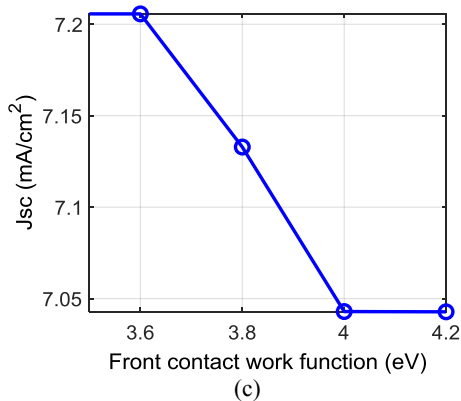
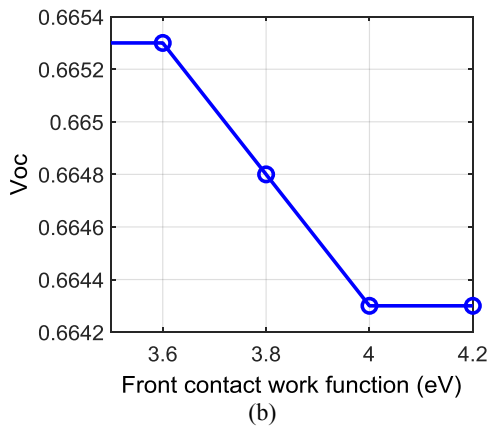
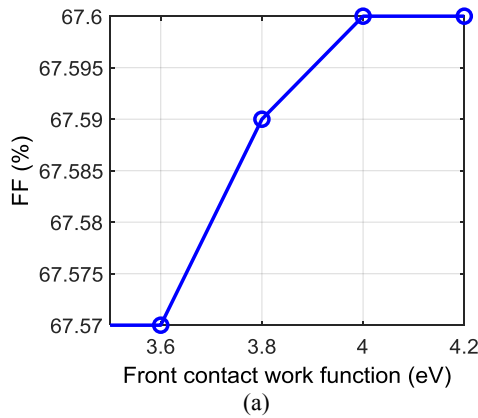
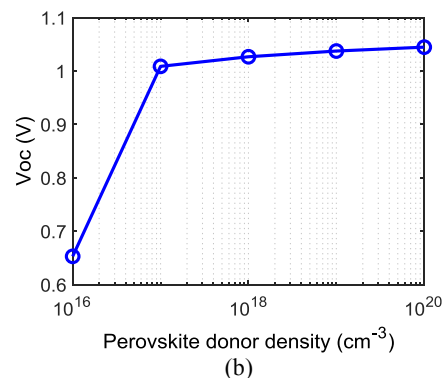
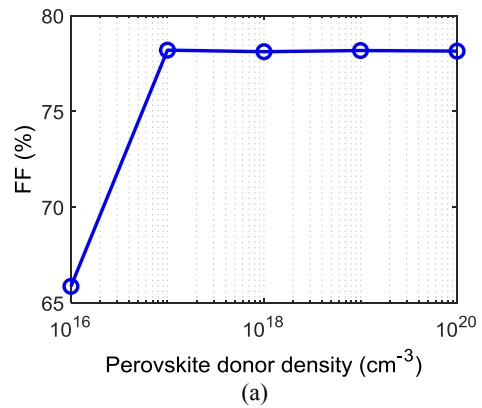


Fig. 13: SnO<sub>2</sub>-based cell performance parameters' variations with the front contact work function thickness (a) FF, (b) V<sub>oc</sub>, (c) J<sub>sc</sub>, and (d) efficiency



d) *Absorber layer optimization:* In the third step to increase efficiency, we worked on the absorber layer (lead-free perovskite) by changing the doping. Figure 14 and Figure 15 show the effect of changing the doping of donors and acceptors of the absorber layer, respectively. Then, we worked on the defect's concentration affecting the absorber layer. The efficiency was 5% with a defect (N<sub>t</sub>) concentration of 10<sup>15</sup> cm<sup>-3</sup> as can be deduced from Figure 16.

Figure 17 shows how the cell's performance parameters are affected by the change in Perovskite thickness. The highest efficiency was 10.13% at an absorber layer thickness of 1.92 μm.





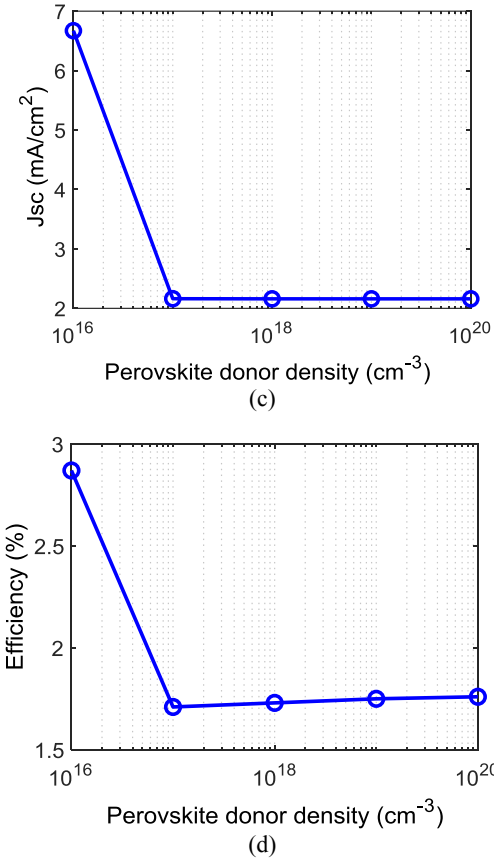


Fig. 14: SnO<sub>2</sub>-based cell performance parameters' variations with the donor's concentration in the absorber layer (a) FF, (b)  $V_{oc}$ , (c)  $J_{sc}$ , and (d) efficiency

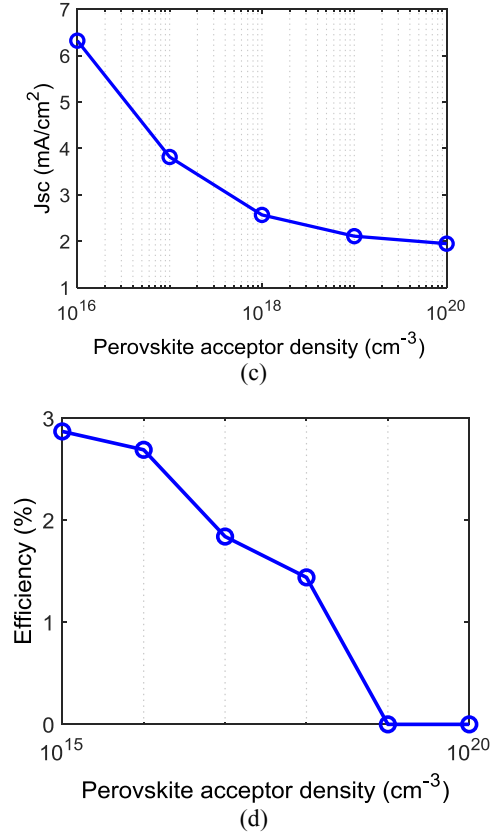
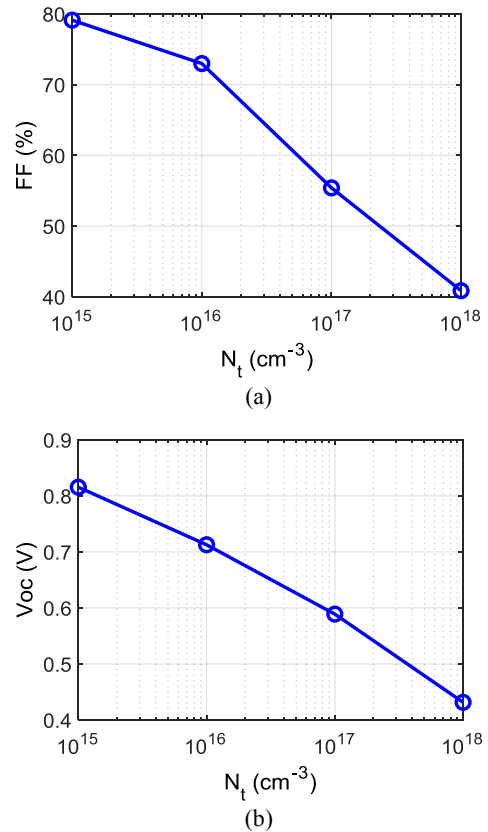
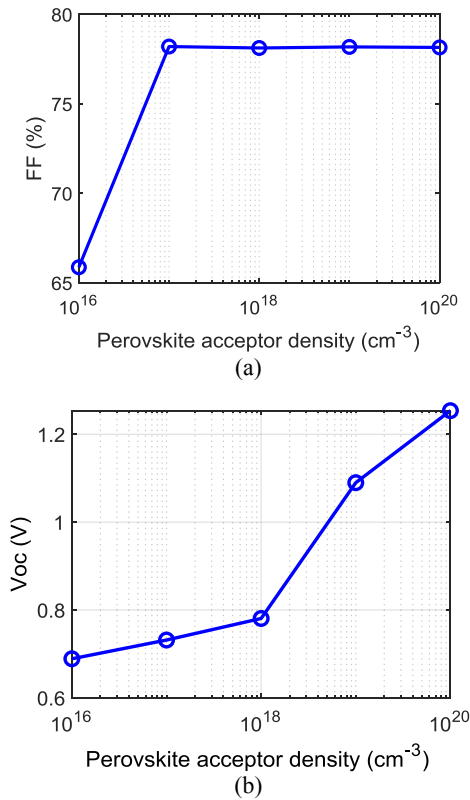


Fig. 15: SnO<sub>2</sub>-based cell performance parameters' variations with the acceptor's concentration in the absorber layer (a) FF, (b)  $V_{oc}$ , (c)  $J_{sc}$ , and (d) efficiency



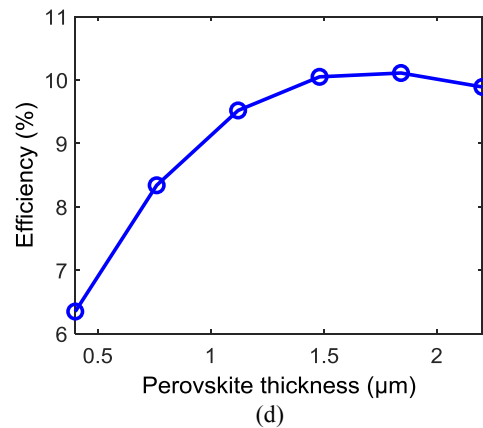
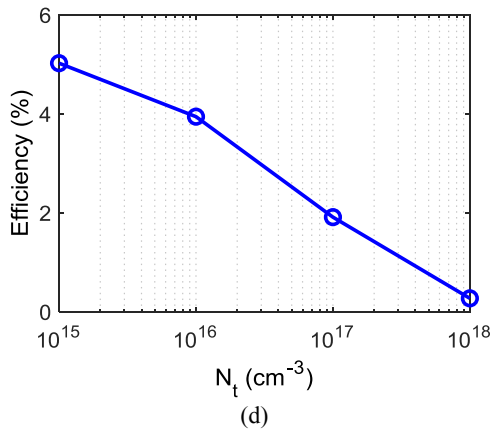
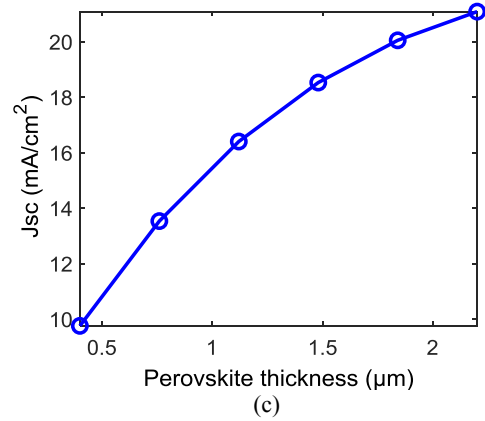
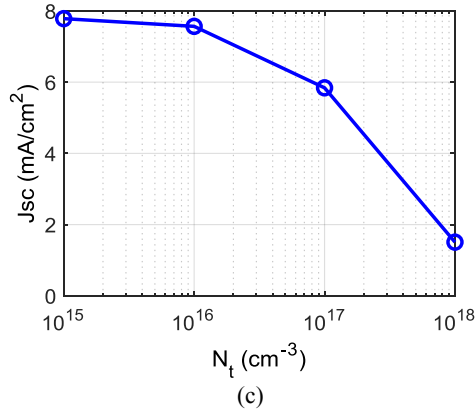
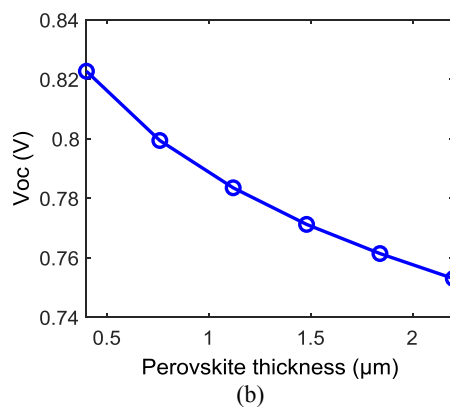
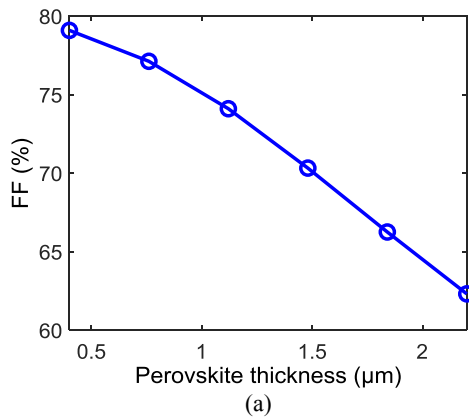


Fig. 16: SnO<sub>2</sub>-based cell performance parameters' variations with the defect density in the absorber layer (a) FF, (b) Voc, (c) JSC, and (d) efficiency

Fig. 17: SnO<sub>2</sub>-based cell performance parameters' variations with the thickness of the absorber layer (a) FF, (b) Voc, (c) JSC, and (d) efficiency



## 4 Conclusion

This theoretical work used SCAPS for analysis. The original design and characteristics of the materials are taken from experimental work. The efficiency and Fill factor of the proposed solar cell are explored and compared when using different ETMs. The highest efficiency happened using SnO<sub>2</sub> material. The efficiency increased from 2.03% to 2.64% besides the fill factor changed from 57.53% to 63.4%.

After changing doping, the thickness of the three layers (ETM, HTM, absorber), the defects concentration ( $N_t$ ) of the Perovskite absorption layer, and the work functions of both front and back contact are optimized. The maximum achieved efficiency was found to be 10.15%.

All things considered, perovskite materials' adaptability and adjustable nature have sparked a great deal of research interest and accelerated advancement in this area in recent years. Sustained progress may result in revolutionary effects in an extensive array of energy and electrical uses. Due to the high efficiency, low-cost manufacturing, and

flexibility of the Lead-free perovskite solar cell, one of the most recommended solar cells to use.

In future work, experimental validation and addressing scalability and stability issues will be investigated.

#### References:

- [1] S. Fouda, M.S. Salem, A. Saeed, A. Shaker, M. Abouelatta, Thirteen-level modified packed u-cell multilevel inverter for renewable-energy applications, *2020 2nd International Conference on Smart Power and Internet Energy Systems, SPIES 2020 (2020)*, 431–435. <https://doi.org/10.1109/SPIES48661.2020.9243059>.
- [2] M. A. M. Shaheen, H. M. Hasanien, R. A. Turky, M. Calasan, A. F. Zobaa, and S. H. E. A. Aleem, “Opf of modern power systems comprising renewable energy sources using improved chgs optimization algorithm,” *Energies (Basel)*, vol. 14, no. 21, 2021, doi: 10.3390/en14216962.
- [3] “Solar Cell: Working Principle & Construction (Diagrams Included), Electrical4U”, 2024, [Online]. <https://www.electrical4u.com/solar-cell/> (Accessed Date: November 18, 2024).
- [4] A. Das, S.D. Peu, M.A.M. Akanda, M.M. Salah, M.S. Hossain, B.K. Das, Numerical Simulation and Optimization of Inorganic Lead-Free-Based Perovskite Photovoltaic Cell: Impact of Various Design Parameters, *Energies (Basel)* 16 (2023). <https://doi.org/10.3390/en16052328>.
- [5] M. Wang, W. Wang, B. Ma, W. Shen, L. Liu, K. Cao, S. Chen, W. Huang, Lead-Free Perovskite Materials for Solar Cells, *Nano-Micro Letters* 2021 13:1 13 (2021) 1–36. <https://doi.org/10.1007/S40820-020-00578-Z>.
- [6] M. Tripathi, V. Vaibhav Mishra, B. S. Sengar, and A. V. Ullas, “Lead-free perovskite solar cell byUsing SCAPS-1D: Design and simulation,” *Mater Today Proc*, vol. 62, pp. 4327–4331, Jan. 2022, doi: 10.1016/J.MATPR.2022.04.832.
- [7] A. Khatibi, F. Razi Astaraei, and M. H. Ahmadi, “Generation and combination of the solar cells: A current model review,” *Energy Sci Eng*, vol. 7, no. 2, pp. 305–322, Apr. 2019, doi: 10.1002/ESE3.292.
- [8] M. Wang et al., “Lead-Free Perovskite Materials for Solar Cells,” *Nano-Micro Letters* 2021 13:1, vol. 13, no. 1, pp. 1–36, Jan. 2021, doi: 10.1007/S40820-020-00578-Z.
- [9] M.S.S. Basyoni, M.M. Salah, M. Mousa, A. Shaker, A. Zekry, M. Abouelatta, M.T. Alshammari, K.A. Al-Dhlan, C. Gontrand, On the Investigation of Interface Defects of Solar Cells: Lead-Based vs Lead-Free Perovskite, *IEEE Access* 9 (2021) 130221–130232. <https://doi.org/10.1109/ACCESS.2021.3114383>.
- [10] B. Lee, A. Krenselewski, S. Il Baik, D. N. Seidman, and R. P. H. Chang, “Solution processing of air-stable molecular semiconducting iodosalts, Cs<sub>2</sub>SnI<sub>6</sub>-xBr<sub>x</sub>, for potential solar cell applications,” *Sustain Energy Fuels*, vol. 1, no. 4, pp. 710–724, May 2017, doi: 10.1039/C7SE00100B.

**Contribution of Individual Authors to the Creation of a Scientific Article (Ghostwriting Policy)**

The authors equally contributed in the present research, at all stages from the formulation of the problem to the final findings and solution.

**Sources of Funding for Research Presented in a Scientific Article or Scientific Article Itself**

No funding was received for conducting this study.

**Conflict of Interest**

The authors have no conflicts of interest to declare.

**Creative Commons Attribution License 4.0 (Attribution 4.0 International, CC BY 4.0)**

This article is published under the terms of the Creative Commons Attribution License 4.0

[https://creativecommons.org/licenses/by/4.0/deed.en\\_US](https://creativecommons.org/licenses/by/4.0/deed.en_US)